

## ORIGINAL ARTICLE

# Gene mapping and candidate gene analysis of a sorghum *sheathed panicle-1* mutant

Jianling Ao<sup>1,2</sup> | Ruoruo Wang<sup>3,4</sup>  | Wenzeng Li<sup>2</sup> | Yanqing Ding<sup>2</sup> | Jianxia Xu<sup>2</sup> | Ning Cao<sup>2</sup> | Xu Gao<sup>2</sup> | Bin Cheng<sup>2</sup> | Degang Zhao<sup>3,4</sup> | Liyi Zhang<sup>2</sup> 

<sup>1</sup>College of life Science, Guizhou University, Guiyang, China

<sup>2</sup>Guizhou Institute of Upland Crops, Guizhou Academy of Agricultural Sciences, Guiyang, China

<sup>3</sup>Plant Conservation Technology Center, Guizhou Key Laboratory of Agricultural Biotechnology, Biotechnology Institute of Guizhou Province, Guizhou Academy of Agricultural Sciences, Guiyang, China

<sup>4</sup>The Key Laboratory of Plant Resource Conservation and Germplasm Innovation in Mountainous Region, Ministry of Education, Guizhou University, Guiyang, China

## Correspondence

Liyi Zhang, Guizhou Institute of Upland Crops, Guizhou Academy of Agricultural Sciences, Guiyang, 550006, China.  
Email: lyzhang1997@hotmail.com

Assigned to Associate Editor Emma Mace.

## Funding information

Guizhou Provincial Basic Research Program (Natural Science), Grant/Award Number: QKH Basic-[2024]Youth 077; Guizhou Provincial Key Laboratory of Biotechnology Breeding for Special Minor Cereals, Grant/Award Number: QKHPT[2025]026; Guizhou Academy of Agricultural Sciences Projects: National Science Foundation by Guizhou Academy of Innovation Capacity Building Project of Guizhou Scientific Institutions, Grant/Award Number: QKFQ[2022]007; Innovation Capacity Building of Guizhou Province Breeding and Scientific Research Foundation Platform, Grant/Award Number: QKHFQ[2022]014; Guizhou Academy of Agricultural Sciences

## Abstract

Panicle exertion is essential for crop yield and quality, and understanding its molecular mechanisms is crucial for optimizing plant architecture. In this study, the *sheathed panicle-1* (*shp-1*) mutant was identified from the ethyl methane sulfonate mutant population of the sorghum [*Sorghum bicolor* (L.) Moench] variety Hongyingzi (HYZ). While phenotypically similar to the wild type during the seedling stage, *shp-1* exhibits a significantly shorter peduncle internode at the heading stage. Cytomorphological analysis revealed reduced parenchyma cell size within the mutant's peduncle internode. Phytohormonal profiling showed lower levels of indole-3-acetic acid and higher concentrations of brassinosteroid in the mutant compared to the wild type at the peduncle internode. Genetic analysis confirmed that the mutant phenotype was caused by a recessive single-gene mutation. Through bulked segregant analysis sequencing (BSA-seq) genetic mapping, the causative locus for the mutant phenotype was localized to a 59.65–59.92 Mb interval on chromosome 10, which contains 28 putative genes. Additionally, the gene *SbiHYZ.10G230700*, which encodes a BTB/POZ and MATH (BPM) domain protein, was identified as a candidate gene. Further analysis revealed that the non-synonymous mutations in the candidate gene were located within the MATH domain, affecting the 3D structure of the protein. In

**Abbreviations:** BPM, BTB/POZ and MATH; BR, brassinosteroid; BSA-seq, bulked segregant analysis sequencing; CYP450, cytochrome P450; ED, Euclidean distance; EMS, ethyl methane sulfonate; *EUI1*, *elongated uppermost internode 1*; GA<sub>3</sub>, gibberellins; GWAS, genome-wide association studies; IAA, indole-3-acetic acid; QTL, quantitative trait locus; *shp-1*, *sheathed panicle-1*; SNP, single-nucleotide polymorphism; *sui*, Chinese pinyin of panicle.

Jianling Ao, Ruoruo Wang, and Wenzeng Li contributed equally to this work.

This is an open access article under the terms of the [Creative Commons Attribution-NonCommercial-NoDerivs License](https://creativecommons.org/licenses/by-nc-nd/4.0/), which permits use and distribution in any medium, provided the original work is properly cited, the use is non-commercial and no modifications or adaptations are made.

© 2025 The Author(s). *The Plant Genome* published by Wiley Periodicals LLC on behalf of Crop Science Society of America.

Key Laboratory Project for Crop Gene Resources and Germplasm Innovation in Karst Mountain regions, Grant/Award Number: QNKZZZY[2023]06; National Science Foundation by Guizhou Academy of Agricultural Sciences, Grant/Award Number: ([2022]03)

summary, this study provides a new genetic material and candidate genes for future research into the molecular regulation of sorghum peduncle length.

### Plain Language Summary

Panicle exertion is crucial for crop yield and quality, and understanding its molecular mechanisms is key to optimizing plant architecture. In this study, a mutant named *sheathed panicle-1* was identified in the sorghum variety Hongyingzi. This mutant, although similar to the wild type at the seedling stage, has a shorter peduncle internode at heading. Cytomorphological analysis showed that the mutant's peduncle internode has smaller parenchyma cells. Genetic analysis revealed that a single recessive gene mutation is responsible for this phenotype. Hormonal profiling showed significant differences in auxin and brassinosteroid levels between the wild type and mutant plants. BSA-seq genetic mapping localized the causative locus to chromosome 10 (59.65–59.92 Mb), containing 28 potential genes. Among these, SbiHYZ.10G230700, which encodes a BTB/POZ and MATH domain-containing protein, was identified as a candidate gene due to non-synonymous mutations affecting its 3D structure.

## 1 | INTRODUCTION

Sorghum [*Sorghum bicolor* (L.) Moench] is the fifth most widely cultivated cereal crop globally. As a C<sub>4</sub> plant, sorghum exhibits strong photosynthetic efficiency, high biomass production, excellent stress tolerance, and broad adaptability, making it particularly suited for planting in the semi-arid and arid regions of Africa and Asia (Baye et al., 2022). As urbanization increases and the rural population ages in China, large-scale cultivation has become a key trend in rural development. Consequently, there is a growing demand for new sorghum varieties tailored for mechanized production to reduce labor and production costs (Fuyao et al., 2019; Shunguo et al., 2021). The culm of graminaceous cereal crops is a crucial organ, primarily composed of multiple internodes interconnected by nodes. The peduncle (PE), also known as the uppermost/first internode (IN1), directly connects to the panicle. The elongation of the PE facilitates the emergence of grain-bearing inflorescences from the flag leaf (FL) sheath, a phenomenon known as panicle exertion. This process is essential for anther dehiscence and pollination, which in turn affects seed set and final grain yield (C. Yin et al., 2007). As a crucial conduit between the panicle sink and other source tissues, the PE plays a vital role in transporting photoassimilates from the FL to the inflorescences, supporting grain filling (Chen & Wang, 2008; Wang et al., 2016). Recent research has demonstrated a significant association between PE elongation and yield-related traits (C. Li et al., 2020). Furthermore, a longer PE can enhance canopy airflow and reduce air humidity, thereby mitigating inflorescences diseases (Jian et al.,

2017). Additionally, the degree of PE elongation can also impact both the loss rate and impurity rate during mechanized sorghum harvesting. Longer PE leads to greater panicle exertion, making mechanized harvesting more efficient (Zhihong et al., 2014).

Most of the current knowledge on the regulation of PE elongation comes from studies on rice. In nearly all male-sterile lines of hybrid rice, the presence of shortened or non-elongating PEs results in sheathed panicles, which block normal pollination and significantly reduce seed production (Shubiao et al., 2005). The *elongated uppermost internode 1 (EUI1)* gene has been identified as the causal gene for the rice sheathed panicle mutant, characterized by a significant elongation of the uppermost internode at the heading stage (Rutger & Carnahan, 1981). *EUI1* encodes cytochrome P450 (CYP450) enzyme, an enzyme responsible for the deactivation of gibberellins (GA<sub>3</sub>). This enzyme specifically deactivates GA<sub>3</sub> in the internode, affecting the degradation of slender rice 1 (SLR1) and the feedback regulation of GA<sub>3</sub> biosynthesis. Overexpression of *EUI1* results in a dwarf phenotype with shorter internodes, a condition that can be partially restored by the application of exogenous GA<sub>3</sub> (Ashikari et al., 1999; Luo et al., 2006). Subsequently, several genes have also been identified and characterized, including *enclosed shorter panicle2* (Guan et al., 2011), *sui1-2* (where *sui* is Chinese pinyin of panicle) (H. F. Yin et al., 2013), *sui1-4* (Fu et al., 2016), *dwarf and sterile plant 1* (Kun, 2009), and *esp1* (Duan et al., 2012). Moreover, a *TaWUS-like* gene associated with PE length has been cloned in wheat (Si et al., 2021). These genes regulate panicle exertion by controlling

the synthesis of plant hormones such as GA<sub>3</sub>, brassinosteroid (BR) and indole-3-acetic acid (IAA). These findings provided valuable insights into the regulation mechanisms underlying the elongation of PE. However, the knowledge regarding PE length in sorghum remains limited. Although 42 quantitative trait loci (QTLs) related to the length of PE have been identified through both biparental mapping and genome-wide association studies (GWAS) (Felderhoff et al., 2012; Feltus et al., 2006; Girma et al., 2019; Perez et al., 2014; Sakhi et al., 2013; Zhao et al., 2016), no candidate genes involved in sorghum panicle exertion have been reported to date.

In this study, we identified a sheathed panicle mutant from the ethyl methane sulfonate (EMS)-mutagenized population of the sorghum variety Hongyingzi (HYZ). By backcrossing with the wild type, we generated an F<sub>2</sub> segregating population and used BSA-seq to map the gene responsible for PE length in sorghum. Through sequence alignment and transcriptome analysis, we identified candidate genes, laying a foundation for further gene cloning and investigation of molecular regulatory mechanisms on sorghum PE elongation.

## 2 | MATERIALS AND METHODS

### 2.1 | Plant materials and phenotypic investigation

A mutant exhibiting shortened PE length, resulting in the panicle being enclosed by the FL sheath and abnormal panicle exertion, was identified from the EMS-mutagenized population of the sorghum variety HYZ (Ding et al., 2020). The mutation was found to be stably inherited no matter planted in Guiyang, Guizhou, or Ledong, Hainan, and the sheathed panicle mutant was designated as *sheathed panicle-1* (*shp-1*). To generate a genetic population, the mutant was used as the female parent to cross with the wild type to obtain the F<sub>1</sub> generation. Then, the F<sub>2</sub> population generated from F<sub>1</sub> self-pollination was used for genetic analysis and BSA-seq. In the spring of 2023, the wild type, mutant, and F<sub>2</sub> populations were cultivated in rows at the experimental field in Guiyang, Guizhou. Each row was 2 m in length, with a spacing of 45 cm between rows and 15 cm between plants. Prior to sowing, 100 kg ha<sup>-1</sup> of compound fertilizer was applied. Standard agronomic practices, including irrigation, fungicide and insecticide application, and other management measures, were followed to ensure optimal plant growth. Upon maturation, the number of plants in the F<sub>2</sub> population with normal panicle exertion was compared to those with sheathed panicles to analyze the segregation ratio. Additionally, 10 wild-type progenies and 10 mutant progenies were randomly selected to evaluate plant height, number of internodes, PE length, the status of panicle exertion, and other agronomic traits.

### Core Ideas

- A novel mutant with a sheathed panicle was identified from the ethyl methane sulfonate-induced mutant population of sorghum cultivar Hongyingzi.
- The mutant exhibits a notable smaller parenchyma cell size in peduncle, caused by improper levels of indole-3-acetic acid and brassinosteroid.
- Genetic analysis revealed that the *sheathed panicle-1* mutant was a recessive mutant caused by a single gene mutation.
- The mutant gene locus was mapped within a 59.65–59.92 Mb region on chromosome 10.
- Additionally, a putative gene encoding a BPM protein has been identified to correlate with the mutant phenotype.

### 2.2 | Cytological analysis of PE internode

A modified approach based on the method proposed by Zou et al. (2024) was utilized for paraffin sectioning to analyze the characterization of parenchyma cells. The PE internode tissues from both the wild type and the mutant were collected during the heading stage, cut into 3 cm segments, and fixed in formalin-acetic acid-alcohol solution (50% ethanol: acetic acid: formaldehyde = 90:5:5) for 24 h. Following this, paraffin sections were prepared and examined microscopically. The same large region of wild type and mutant paraffin sectioning was scanned to quantify cell numbers, and the dimensions of the parenchyma cells were measured using CaseViewer software (Version 2.4.0, <https://www.3dhitech.com/solutions/caseviewer/>).

### 2.3 | Detection of phytohormones

Panicles, PEs, and leaf sheath samples from both wild type and mutant plants were collected on the fourth day after panicle exertion, with three replicates for each sample. After rapid freezing in liquid nitrogen, the levels of GA<sub>3</sub>, IAA, and BR were detected using liquid chromatography-tandem mass spectrometry (LC-MS/MS) (Sheflin et al., 2019).

### 2.4 | DNA extraction and BSA-seq

The F<sub>2</sub> population was used to select individuals with extreme phenotypes. After heading, 30 lines with normal panicle exertion and 30 lines with sheathed panicles were selected for DNA extraction using the cetyltrimethylammonium bromide method (Murray & Thompson, 1980). DNA from

each group was pooled in equal molar amounts to construct the wild type and mutant pools, designated as WT and MT, respectively. Additionally, 10 plants from each parental line (wild type and mutant) were selected, and their DNA was extracted using the same method. The parental DNA was then pooled in equal molar amounts to construct the parental pools, designated as P-WT and P-MT. Four DNA libraries were prepared following the standard protocols of Beijing Genomics Institute (BGI). Genomic DNA was fragmented using ultrasonic shearing, followed by end-repair, 3' A-tailing, adaptor ligation, and PCR enrichment. Whole-genome resequencing (150 bp paired-end) was performed on the BGISEQ-T7 platform (BGI Genomics).

The raw sequencing data were processed using Soap-nuke (Version 1.65) for quality control and filtering. This involved removing adapter-contaminated reads, low-quality reads ( $\geq 20\%$  bases with a quality score  $\leq 15$ ), and reads with  $>5\%$  N content. The resulting high-quality clean data were used for subsequent analysis. The clean data were aligned to the HYZ reference genome (Ding et al., 2024) using the “mem” algorithm of BWA software (Version 0.7.15-r1140). The alignment results were sorted with SAMtools software (Version 1.9). Single-nucleotide polymorphism (SNP) and InDel variant detections were performed using the HaplotypeCaller algorithm based on GATK software (Version 4.1.2) (McKenna et al., 2010). The variant sites were annotated and predicted using SnpEff software (Version 5.1). The sequencing depth, genome coverage, and other relevant metrics were calculated using PanDepth software (Version 1.0).

The SNP-index and  $\Delta$  (SNP-index) were computed across all chromosome positions using a sliding window of 1 Mb and a step size of 500 kb. A SNP index value of 0 indicates there is no variation, a SNP index value of 1 indicates all SNPs belong to either parent, and a SNP index value of 0.5 indicates each parent contributes equally to the variation. A distribution graph of  $\Delta$  (SNP-index) across chromosomes was then generated. Additionally, the Euclidean distance ( $ED$ ) algorithm was implemented to evaluate differences in base frequencies between the T-pool and S-pool at each SNP locus. To further enhance the signal-to-noise ratio and reduce background noise, the  $ED$  value was raised to the 4th power ( $ED^4$ ). The  $ED$  for each SNP locus was calculated using the following formula (Wu et al., 2020):

represent the frequencies of bases  $A$ ,  $C$ ,  $G$ , and  $T$  in the wild-type pool. To amplify the differences and reduce background noise, the  $ED$  value was raised to the 4th power ( $ED^4$ ) as follows (Zhang et al., 2019):

$$ED^4 = \left[ (A_{aa} - A_{ab})^2 + (C_{aa} - C_{ab})^2 + (G_{aa} - G_{ab})^2 + (T_{aa} - T_{ab})^2 \right]^2$$

The  $ED^4$  algorithm was implemented using a custom Python program. The software environment included Python (Version 3.8) and essential libraries such as NumPy and Pandas for efficient mathematical operations and data handling. The intersection of significant results from SNP-index and  $ED^4$  was used to pinpoint candidate regions associated with PE length traits, with a selection threshold set as a 99% confidence level.

## 2.5 | Transcriptome sequencing

Samples were collected from wild type and mutant sorghum plants at two developmental stages: S1 (booting stage) and S2 (4 days after heading), focusing on the PE, FL, and panicle (P). At the S1 stage, the panicle was still immature and enclosed within the leaf sheath. The panicle was collected from the point of the most prominent bulge within the sheath. It was carefully removed from the sheath and separated from the PE for sampling. At the S2 stage, the panicle of the wild-type plants had fully emerged from the sheath, while the panicle of the mutant plants remained partially enclosed. For consistency, the uppermost mature part of the panicle was collected for both genotypes. Although the panicle was more developed at this stage, it had not yet flowered, and therefore, no seeds were included in the samples. Three biological replicates were established for each developmental stage, and total RNA was extracted from the different tissues at each time point using TRIzol Reagent (Invitrogen). Transcriptome libraries were constructed utilizing the TruSeq RNA Library Prep Kit (Illumina) according to the manufacturer's protocol, followed by high-throughput sequencing conducted on the Illumina NovaSeq 6000 platform. Sequencing quality was assessed using Trimmomatic software (Version 0.39) (Bol-

$$ED = \sqrt{(A_{aa} - A_{ab})^2 + (C_{aa} - C_{ab})^2 + (G_{aa} - G_{ab})^2 + (T_{aa} - T_{ab})^2}$$

where  $A_{aa}$ ,  $C_{aa}$ ,  $G_{aa}$ , and  $T_{aa}$  represent the frequencies of bases  $A$ ,  $C$ ,  $G$ , and  $T$  in the mutant pool.  $A_{ab}$ ,  $C_{ab}$ ,  $G_{ab}$ , and  $T_{ab}$

ger et al., 2014) to remove adapters, and the clean data were aligned to the HYZ reference genome using hisat2 software

(Version 2.2.1) (Kim et al., 2019). The Cufflinks software (Version 2.2.1) (Trapnell et al., 2012) is utilized to assemble transcripts, estimate their abundance, and assess differential expression between samples. The transcripts levels were calculated by FPKM (fragments per kilobase of transcript per million mapped reads).

## 2.6 | Selection of candidate genes

Utilizing the HYZ reference genome and its associated annotation data, candidate genes located within the BSA-mapped regions were identified and the mutation sites in the exon of candidate genes were verified in the variant call format (vcf) file. Subsequently, the expression levels of mutational candidate genes were then evaluated in the transcriptome data. Integrating BSA-seq, gene mutation verification, and transcriptome gene expression analysis, genes in the candidate region with mutations in coding regions and different expression between mutant and wild type were filtered to identify candidate genes. Meanwhile, BLAST analysis of genes with non-synonymous and frameshift mutations was conducted in public databases, including those for rice (<https://ricerc.sicau.edu.cn/>), maize (<https://www.maizegdb.org/>), and wheat (<https://www.wheatgenome.org/>), to search their homolog genes and corresponding gene function.

## 2.7 | Protein structure prediction

Protein sequences of candidate genes were extracted based on the annotation of HYZ reference genome, and their conserved domains were identified using the InterPro website (<https://www.ebi.ac.uk/interpro/>). The mutational protein sequences were substituted based on the mutation information in vcf file. AlphaFold (Version 2.3.2) (Jumper et al., 2021) was used to predict the monomer type of protein structure using all multiple sequence alignment database to optimize the best model.

## 2.8 | Data processing and statistical analysis

Descriptive statistical analysis and Student's *t*-test were conducted using SPSS software (Version 22.0), with a significance level set at  $p < 0.05$ .

# 3 | RESULTS

## 3.1 | Phenotypic analysis of the *shp-I* mutant

To acquire mutants with atypical PEs, we performed a phenotypic assessment of the EMS-mutagenized HYZ population and successfully identified the *shp-I* mutant with signifi-

cantly reduced PE length. The mutant underwent multiple generations of self-pollination and field evaluations conducted in Guiyang, Guizhou, and Ledong, Hainan. Phenotypic assessments conducted throughout the developmental period revealed a significant difference in plant height between the wild type and the mutant was observed ( $244 \pm 2.0$  cm vs.  $176 \pm 3.93$  cm, respectively), especially in PE length ( $174 \pm 1.03$  cm vs.  $158 \pm 1.78$  cm, respectively) (Figure 1A; Table 1). During the heading stage, the wild type exhibited normal PE exertion, while the mutant displayed inadequate PE elongation (Figure 1B). At maturity, both genotypes had a similar number of internodes. However, the *shp-I* mutant showed a significant reduction in internode length from the PE to the third internode (IN1 to IN3), with the PE length decreasing by up to threefold (Figure 1C,D), which suggests that the shorter PE length in the mutant is the primary factor contributing to its mature height. Additionally, the length of panicle exertion was  $22.92 \pm 1.58$  cm in the wild type, while in the mutant, 36.73% of the panicles were covered by the FL sheath, resulting in a negative exposed panicle length of  $-11.16 \pm 1.39$  cm (Figure 1E). Furthermore, the mutant also exhibited a notable reduction in panicle length, thousand-grain weight, grain length, and grain width (Table 1).

## 3.2 | Morphological observation of mutant PE cells

To investigate the potential cellular basis underlying the significant shortening of PE length, which contributes to the sheathed panicle phenotype, we conducted microscopic observations on the longitudinal sections of PE internodes in both the wild type and the mutant during the heading stage. The results indicated that the average cell length in the mutant was reduced by 59.43% compared to the wild type, demonstrating a highly significant difference (Figure 2A,B,C). Additionally, the average cell width in the mutant showed a 40.56% reduction compared to the wild types, which again showed a highly significant difference (Figure 2D). On the contrary, the numbers of parenchyma cells in PE are more than that of wild type (Figure 2E). These cytological observations imply that the shortening of the PE length is due to the failure of parenchyma cells to elongate and expand.

## 3.3 | Analysis of phytohormone concentrations in mutants

Previous reports have demonstrated that phytohormones can influence the elongation and expansion of PE, including GA<sub>3</sub>, IAA, and BR. To ascertain whether the concentrations of those phytohormones were altered in the mutant, we quantified the concentrations of GA<sub>3</sub>, IAA, and BR in panicles,

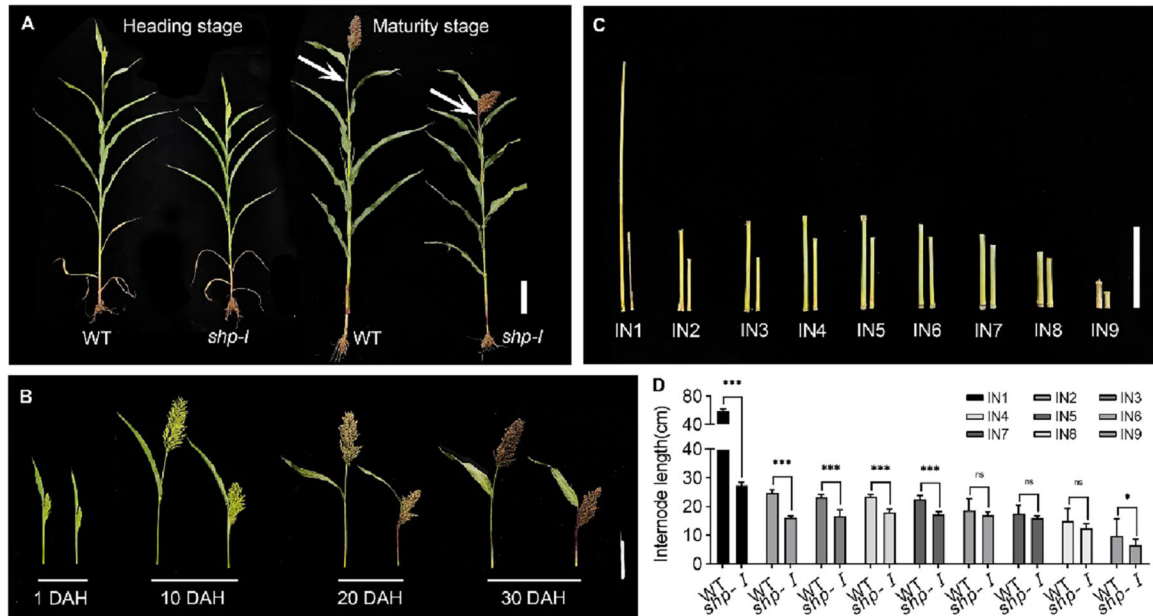


**FIGURE 1** Phenotypic analysis of wild type and *sheathed panicle-1* (*shp-1*) mutant. (A) Phenotypes of wild type and mutant at heading and maturity stages. The white arrows indicate the panicle exertion status in wild type and mutant. (B) Panicle exertion status of the wild type (left) and the mutant (right) at different development stages. DAH, day after heading. (C) Internodes of wild type (left) and the mutant (right) at maturity stage. IN1 to IN9 denote the first internode to the ninth internode from the apex to the base of plant morphology. (D) The quantification of internode lengths between the wild type and the mutant (\*\* $p < 0.001$ , two-sided unpaired Student's *t*-test). Data presents mean  $\pm$  SD ( $n = 10$ ). Scale bars in A, B, and C are 20 cm.

**TABLE 1** Comparison of agronomic traits between wild type and mutant variants.

Agronomic trait	Mutant	Wild type	Difference(%)
Plant height at booting stage(cm)	158 $\pm$ 1.78	174 $\pm$ 1.03	-9.19**
Plant height (cm)	176 $\pm$ 3.93	244 $\pm$ 2.0	-27.86**
Flag leaf length (cm)	7.52 $\pm$ 0.45	7.8 $\pm$ 0.29	-3.58
Ear length (cm)	31.58 $\pm$ 0.96	34.68 $\pm$ 2.07	-8.93**
1000-Grain weight (g)	22.47 $\pm$ 0.78	26.01 $\pm$ 0.21	-13.61**
Seed length (mm)	4.47 $\pm$ 0.03	4.65 $\pm$ 0.02	-3.87**
Seed width (mm)	3.57 $\pm$ 0.03	3.72 $\pm$ 0.01	-4.03**
Internode numbers	9	9	0

Note: The data in the table are presented as "mean  $\pm$  standard deviation."

\*\*Statistically significant difference at  $p < 0.01$  level.

PEs, and FL, of the wild type and mutant on the fourth day after heading when the panicles of the mutant emerged with a similar length to the wild type (Figure 3). The GA<sub>3</sub> levels were consistently low in three tissues of both the wild type and mutant plants, with no significant difference observed in PEs. IAA levels were highest across all tissues, showing significant differences; levels were higher in wild-type PEs compared to mutants, but lower in the wild-type panicles and leaf sheaths compared to mutants. BR levels showed no sig-

nificant difference in panicles between the two genotypes but were significantly lower in wild-type PEs and higher in wild-type leaf sheaths compared to mutants. These results suggest that the levels of IAA and BR likely influence the elongation of sorghum PEs.

### 3.4 | Genetic analysis of the mutant

Upon crossing the mutant with wild type, the F<sub>1</sub> generation exhibited the wild-type phenotype, indicating that the mutant trait is inherited recessively. Analysis of 247 F<sub>2</sub> progeny revealed 183 individuals with normal PE elongation and 64 individuals exhibiting aberrant PE elongation, yielding a segregation ratio close to 2.85:1. Chi-square testing confirmed that the observed ratio aligns with the expected 3:1 Mendelian ratio, with  $\chi^2_{0.05}(1) = 0.1093 < \chi^2_{0.05}(1) = 3.84$  (Table 2), indicating that the mutant phenotype is controlled by a single recessive gene.

### 3.5 | BSA-seq analysis of F<sub>2</sub> generation and candidate gene identification

To identify candidate genes associated with the mutant phenotype, we conducted BSA-seq analysis using F<sub>2</sub> populations of mutant and wild-type individuals. Sequencing generated 281,057,654 reads (49.33 $\times$ ) for wild type and 443,960,400

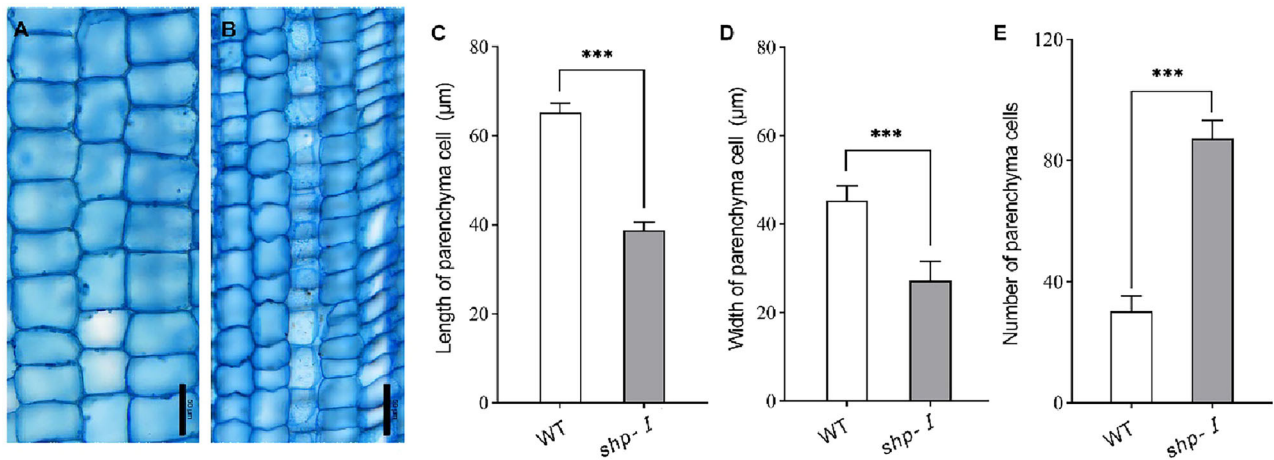


**FIGURE 2** Morphological analysis and the quantification of parenchyma cells dimensions and quantities within the longitudinal section of peduncle. (A) Visual field of randomly selected parenchyma cells within the peduncle of wild type. (B) Visual field of randomly selected parenchyma cells within the peduncle of mutant. Scale bars in A and B are 50 μm. (C) The length of parenchyma cells in wild type and mutant. (D) The width of parenchyma cells in wild type and mutant. (E) The number of pith parenchyma cells in the same visual field. \*\*\*Statistically significant difference at the  $p < 0.001$  level.

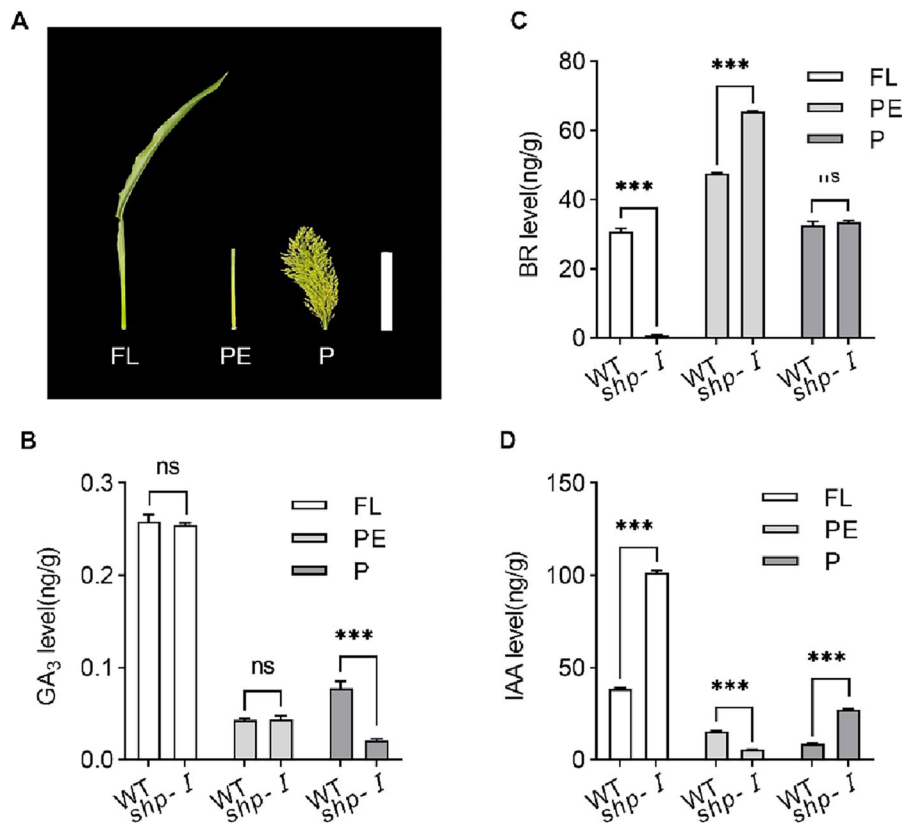


**FIGURE 3** (A) Isolated tissues utilized for the quantification of phytohormone levels. FL, flag leaf; PE, peduncle; P, panicle. (B) The concentrations of gibberellins (GA<sub>3</sub>) in different tissues of wild type and mutant. Scale bar in A is 20 cm. (C) The concentrations of brassinosteroid (BR) in different tissues of wild type and mutant. (D) The concentrations of indole-3-acetic acid (IAA) in different tissues of wild type and mutant. \*\*\*Statistically significant difference at  $p < 0.001$  level.

**TABLE 2** Chi-square test for phenotypic segregation in F<sub>2</sub> populations.

	NPE	APE	Total number	Segregation ratio	$\chi^2$
Observed value	183	64	247	2.85:1	0.1093
Expected value	185.25	61.75		3:1	

Abbreviations: APE, abnormal panicle exertion; NPE, normal panicle exertion.

**TABLE 3** Statistics of sequencing data.

Sample type		Mean depth	Cleanreads	Cleanbase	GC (%)	Q30 (%)	Mapped reads (%)
Parents	HYZ	49.23×	281,057,654	42,158,648,100	43.56	90.23	99.22
	Mutant	72.74×	443,960,400	66,594,060,000	43.80	91.63	95.27
F2	Sheathed panicle	35.02×	208,165,308	31,224,796,200	43.79	88.39	97.21
	Normal panicle exertion	53.99×	322,975,058	48,446,258,700	44.02	89.95	97.54

Abbreviation: HYZ, Hongyingzi.

reads (72.74×) for mutants (Table 3). Pooled sequencing of F<sub>2</sub> population yielded 208,165,308 reads (35.02×) for wild type and 322,975,058 reads (53.99×) for mutants (Table 3). Across the four pooled sequencing libraries, the mean percentage of bases with quality scores 30 (Q30) was 90.05%, and the average GC content was 43.79%. Re-sequenced data of wild-type library exhibited a mapping alignment rate of 99.22% when aligned with the T2T reference genome of HYZ. Moreover, the remaining three sequencing libraries showed an average mapping rate of 96.67%, with lowest rate recorded at 95.27%. These results demonstrate that the resequencing data quality across the four libraries is robust, rendering them appropriate for subsequent BSA-seq evaluations. In total, 836,507 SNPs and 207,726 InDel variant sites were identified across the four sample pools. Using the  $\Delta$ -SNP-index algorithm, a significant candidate region of 0.29 Mb (59.65–59.94 Mb) on chromosome 10, encompassing 32 genes, was detected (Figure 4A). Subsequently, employing the ED<sup>4</sup> algorithm identified two significant candidate regions on chromosomes 9 and 10, with lengths of 1.02 Mb (60.93–61.68 Mb) and 0.27 Mb (59.65–59.92 Mb), respectively, including 128 annotation genes (Figure 4B). After intersecting the results of candidate regions from both algorithms, a 0.27 Mb candidate interval (59.65–59.92 Mb) on chromosome 10 was pinpointed. Using T2T genome of HYZ as a reference, we found 28 genes were within the 0.27 Mb candidate interval, among which six genes (viz., *SbiHYZ.10G230300*, *SbiHYZ.10G230600*, *SbiHYZ.10G230700*, *SbiHYZ.10G230900*, *SbiHYZ.10G231000*, and *SbiHYZ.10G231600*) contained non-synonymous mutations in their exons (Table 4).

Subsequent BLAST alignment and functional annotation of these six genes against rice, maize, and wheat (Table 5) revealed that five of these genes (namely *SbiHYZ.10G230300*, *SbiHYZ.10G230600*, *SbiHYZ.10G230700*, *SbiHYZ.10G230900*, and *SbiHYZ.10G231000*) encode the BTB/POZ and MATH (BPM) domain-containing proteins and are homologous to the *LOC\_Os06g45720*,

*Zm00001d036646*, *Zm00001d036643*, and *Zm00001d036641* in rice and maize, respectively (Table 5). The proteins encoded by these five genes are integral components of the E<sub>3</sub> ubiquitin ligase complex. Given their significant involvement in hormone-mediated signal transduction, these five genes were designated as candidate genes for further investigation.

### 3.6 | Expression levels of candidate genes in wild type and mutant

To further detected the candidate gene expression levels in the mutant and wild type, we collected sample from the FL, PEs, and panicles at the fourth day (S1) and the 10th day (S2) after heading to perform an RNA-seq analysis. Among the candidates, *SbiHYZ.10G230700* showed higher expression levels in the mutant compared to the wild type in various tissues and stages, with the highest expression observed in the PE at both stages. In contrast, the other four candidates (*SbiHYZ.10G230300*, *SbiHYZ.10G230600*, *SbiHYZ.10G230900*, and *SbiHYZ.10G231000*) were not expressed in any tissues of either the wild type or mutant at both stages (Figure 5). Based on these findings, *SbiHYZ.10G230700* is identified as key candidate genes.

### 3.7 | Protein structure prediction of candidate genes

Disruption in the genetic encoding of protein structures can affect gene function. To evaluate whether non-synonymous mutations in the candidate gene impact the function of the encoded proteins, we analyzed the amino acid sequences of the proteins encoded by the candidate gene and their corresponding sequences in the mutants. The non-synonymous mutation sites in *SbiHYZ.10G230700* (G to C, G to A, C to G, A to T, and A to T) were identified at the 41st,

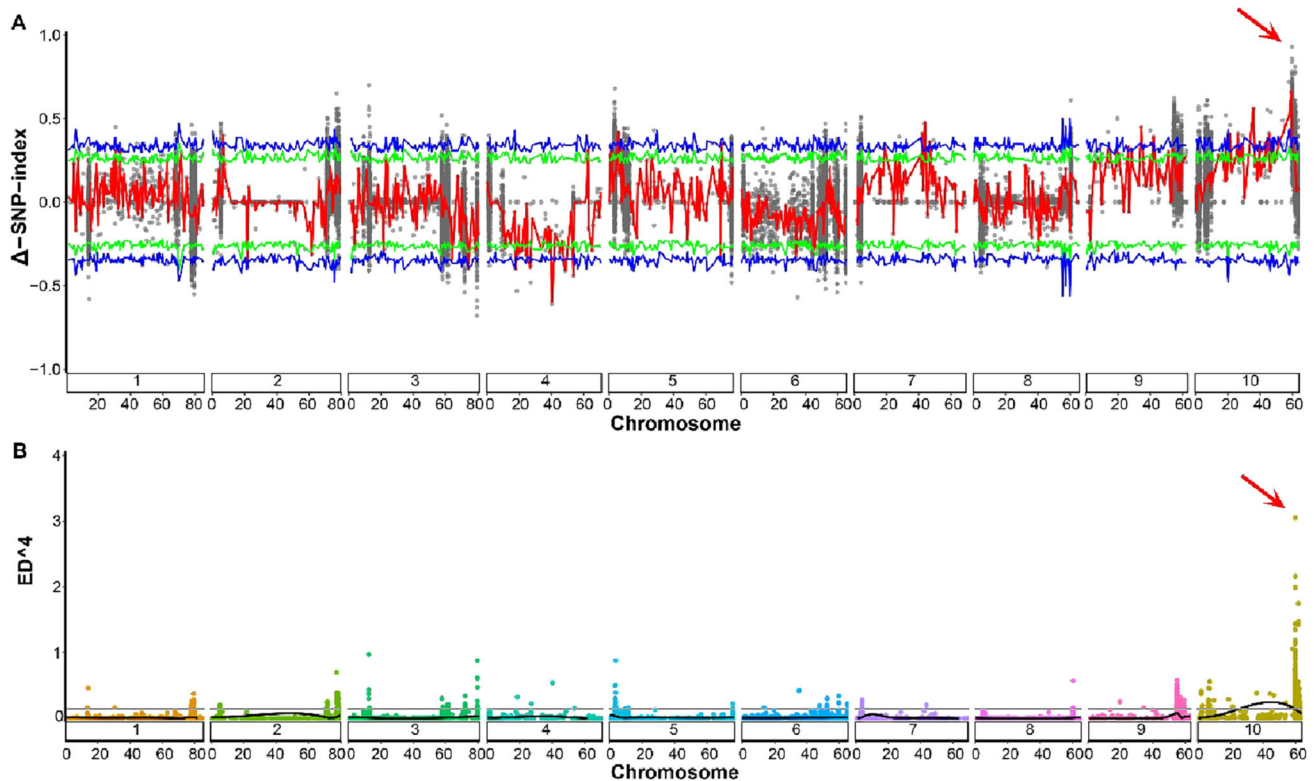


**FIGURE 4** The BSA-seq analysis of  $F_2$  population derived from mutant ( $\text{♀}$ ) and wild type ( $\text{♂}$ ). (A) Manhattan Plot generated based on single-nucleotide polymorphism (SNP)-index algorithm. The X-axis represents the chromosomes of the reference genome, and the Y-axis denotes the  $\Delta$ SNP index value between the mutant and wild-type pools. The blue and green lines indicate the 99% and 95% confidence intervals, respectively. The black dots denote the  $\Delta$ SNP-index for each SNP, and the red line is the fitted curve of the mean values of  $\Delta$ SNP-index derived from the sliding window analysis. The red arrow indicates the peak above the threshold on the Chromosome 10. (B) Manhattan Plot generated based on Euclidean distance (ED) algorithm. The X-axis represents the chromosomes of the reference genome, the Y-axis denotes the  $ED^4$  value. The grey line represents the 99% threshold; the black line is the fitted curve of the  $ED^4$  values. The red arrow indicates the candidates significantly above the threshold. BSA-seq, bulked segregant analysis sequencing.

45th, 60th, 76th, and 79th amino acid positions, resulting in the following amino acid substitutions: D41V, Q45H, D60E, R76Q, and G79R (Figure 6A; Table 4). Furthermore, the mutated amino acid sites in the candidate gene are situated within the conserved MATH domain of the encoded proteins (Figure 6A). Structural predictions using AlphaFold 2.3.2 revealed that the protein structures encoded by the candidate gene differ between the wild type and the mutants, the N-terminus and C-terminus exhibited significant structural changes (Figure 6B).

## 4 | DISCUSSION

### 4.1 | The shortened PEs of *shp-I* mutants are mainly due to the block of the parenchyma cells elongation

The elongation of crop PE not only affects the plant height but also relates to the degree of panicle exposure, which is cru-

cial for the grains harvest yield (McKim, 2019). In sorghum, a severe reduction in PE length can lead to increased loss and impurity rate during mechanized harvesting. In this study, the mutant with significantly shortened PE length obtained by EMS-mutagenized resulted in a significant reduction in panicle exertion, with parts of panicles being enveloped by the leaf sheaths of the flag leaves, resulting in partially sheathed panicle. Moreover, the mutant exhibited significantly lower values in key traits such as plant height, panicle length, internode length, 1000-grain weight, grain length, and grain width compared to the wild type. Parenchyma cell elongation is crucial for internode elongation in plants. Examination of the longitudinal section of slices of the PE revealed that both the length and width of the mutant's parenchyma cells were significantly reduced compared to the wild type. Similar results were also observed in the sheathed panicle mutants *sui2*, *sui1-5*, and *OsWRKY78* in rice, indicating that the reduced PE length of grass mutants is mainly due to the compromised extensibility of the PE's parenchyma cells (Mei et al., 2024; Qi et al., 2020; Ye et al., 2023).

**TABLE 4** The non-synonymous mutations sites and the associated amino acid residues in the six candidate genes.

Gene name	Variant position	DNA		Amino acid	
		REF	ALT	REF	ALT
<i>SbiHYZ.</i>	59,790,017	C	A	P	T
<i>10G230300</i>	59,790,066	G	T	E	D
	59,790,071	A	C	I	L
	59,790,088	G	A	C	Y
	59,790,152	A	G	I	V
	59,790,208	T	A	V	E
	59,790,305	A	G	N	D
	59,790,344	G	A	D	N
	59,790,349	T	A	F	Y
	59,790,352	G	T	W	L
	59,790,353	T	G	W	
<i>SbiHYZ.</i>	59,809,655	C	T	S	F
<i>10G230600</i>	59,809,833	G	C	A	P
<i>SbiHYZ.</i>	59,812,575	G	C	G	R
<i>10G230700</i>	59,812,583	G	A	R	Q
	59,812,630	C	G	D	E
	59,812,675	A	T	Q	H
	59,812,688	A	T	D	V
<i>SbiHYZ.</i>	59,826,099	A	T	K	M
<i>10G230900</i>	59,826,229	A	G	N	D
	59,826,232	G	A	D	N
	59,826,235	A	T	N	Y
<i>SbiHYZ.</i>	59,832,237	T	G	L	V
<i>10G231000</i>	59,844,985	C	T	R	C
<i>SbiHYZ.</i>	59,883,675	A	G	K	E
<i>10G231600</i>					

Abbreviations: ALT, alternative sequence; REF, reference sequence.

## 4.2 | The biosynthesis and transduction of BR and IAA play crucial roles in the sorghum panicle exertion

Numerous studies on the genetic mechanisms underlying the sheathed panicle in rice have demonstrated that PE length is intricately linked to the synthesis and regulation of plant hormones (such as GA<sub>3</sub>, IAA, and BR). GA<sub>3</sub> plays a crucial role as a key phytohormone in regulating cell elongation and internode length (Tong & Chu, 2018). For instance, the *EUII* gene encodes a P450 monooxygenase, which regulates internode elongation by modulating the GA<sub>3</sub> response in rice (Luo et al., 2006; Y. Zhu et al., 2006). The transcription factor *OsWRKY78* regulates the expression of genes involved in GA<sub>3</sub> biosynthesis and metabolism, resulting in sheathed panicle phenotypes in its mutants (Mei et al., 2024). However, in this study, we found no significant difference in GA<sub>3</sub> concentrations within the PE tissues of the wild type and mutant,

suggesting that the phenotypic characteristics of the *shp-1* mutant may not be directly related to GA<sub>3</sub>.

In addition to GA<sub>3</sub>, BR is also a plant hormone that promotes cell elongation. The typical synthesis-deficient mutant *det2* and the signal-insensitive mutant *bri1* exhibit phenotypes characterized by shortened hypocotyls and dwarfism (X. Chen et al., 2024; Friedrichsen & Chory, 2001). Similarly, the *Osbri1* mutant in rice also demonstrates significant phenotypes, including shortened internodes and reduced lengths of parenchyma cells (Yamamuro et al., 2000). In wheat, the absence of *ZnF-B* leads to shortened internodal parenchyma cells due to impaired perception of BR, resulting in a semi-dwarf phenotype in the plants (Song et al., 2023). In rice, *sui2* encodes a CYP450 protein involved in BR synthesis, participating in the developmental regulation of the PE by modulating BR biosynthesis. *Sui1-5* encodes endo-1,4-β-glucanase, which is hypothesized to be involved in the regulation of cell wall synthesis and the extension of the PE. BR may regulate cell elongation by modulating the formation, orientation, and remodeling of microtubules and the cell wall (X. Chen et al., 2024; Rao & Dixon, 2017; Xiong et al., 2021). Recent studies have reported that BR promote the demethylesterification of pectin in the cell wall, leading to isotropic relaxation of the planar cell wall and contributing to the morphological development of plant organs (Xiong et al., 2021). *OsWRKY78*, a member of the WRKY gene family, regulates the development of the PE by directly modulating GA biosynthesis and indirectly regulating GA metabolism while also participating in the regulation of BR signal transduction. Consequently, among the previously reported genes responsible for PE length (Table S1), such as *sui2*, *sui1-5*, and *OsWRKY78*, which are directly or indirectly related to BR. In this study, the concentration of BR in mutant is significantly higher than that in the wild type, which is negative with the PE length. The synthesis of BR is subject to negative feedback regulation to maintain homeostasis within the plant (Tanaka et al., 2005). When BR signaling is disrupted, the feedback inhibition of key BR biosynthetic genes such as *DWF4* and *CPD* by *BES1/BZR1* is relieved (Guo et al., 2023; He et al., 2005; Tanaka et al., 2005), exemplifying the well-known feedback mechanism—defects in BR signaling typically lead to an increase in BR synthesis. Previous studies have elucidated the complex crosstalk between the plant hormones BR and auxin, encompassing both synergistic and antagonistic interactions (Guo et al., 2024; Tian et al., 2018). Notably, some target genes within the BR and auxin signaling pathways share common regulatory elements (Halliday, 2004). BR is capable of regulating the biosynthesis, polar transport, and translocation processes of auxin (Guo et al., 2024). Conversely, auxin can also regulate BR synthesis and signaling. In light of the phenotypic characteristics of the mutants and the hormone concentration measurement results, we hypothesize that the severely shortened PE phenotype of the mutant is likely due

**TABLE 5** Genomic localization and the functional annotation of six candidate genes.

Gene ID	Physical position	Homolog genes	Functional annotation	Similarity(%)
<i>SbiHYZ.10G230300</i>	59,789,257–59,790,521	<i>LOC_Os06g45720</i>	BTB/POZ domain containing protein	46
<i>SbiHYZ.10G230600</i>	59,808,979–59,810,362	<i>Zm00001d036646</i>	Broad complex BTB domain with Meprin and TRAF homology MATH domain	52
<i>SbiHYZ.10G230700</i>	59,811,377–59,813,244	<i>LOC_Os08g13030</i>	Broad complex BTB domain with Meprin and TRAF homology MATH domain	72
<i>SbiHYZ.10G230900</i>	59,825,261–59,826,400	<i>Zm00001d036641</i>	Broad complex BTB domain with Meprin and TRAF homology MATH domain	61
<i>SbiHYZ.10G231000</i>	59,831,207–59,832,662	<i>Zm00001d036641</i>	Broad complex BTB domain with Meprin and TRAF homology MATH domain	60
<i>SbiHYZ.10G231600</i>	59,881,451–59,886,823	<i>Zm00001d046973</i>	Conserved oligomeric Golgi complex component 7	97

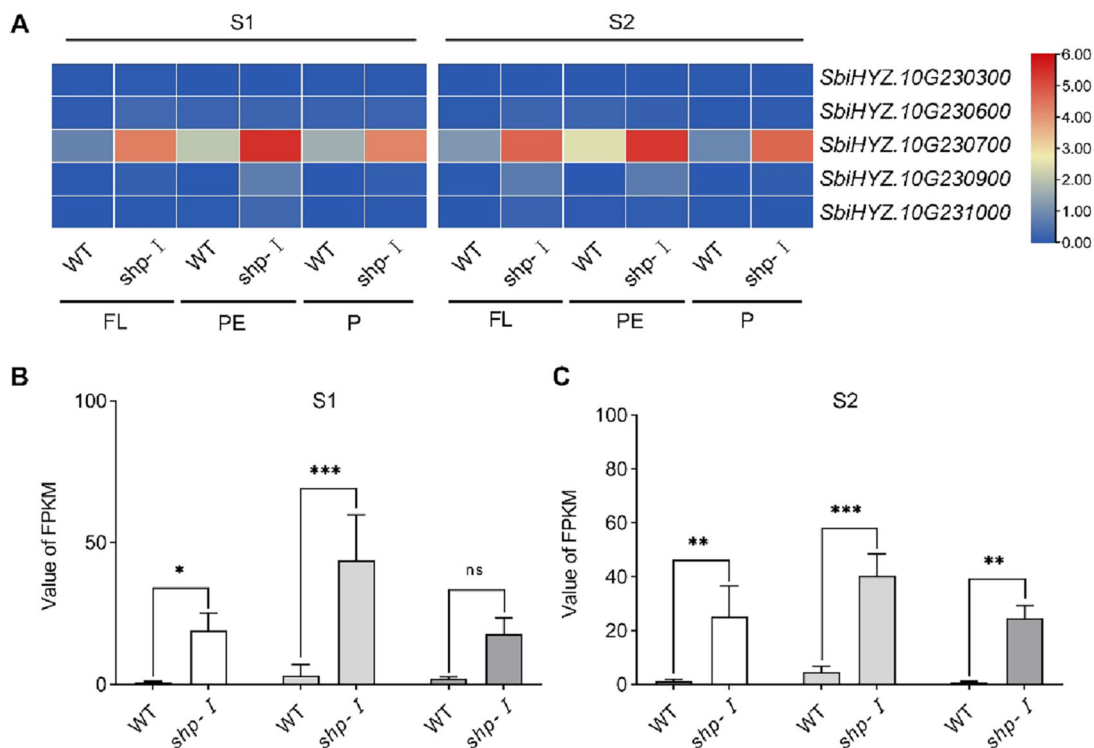


**FIGURE 5** The expression levels of five candidate BTB/POZ and MATH (BPM) domain-containing genes in flag leaf, peduncle, and panicle at two development stages in wild type and mutant. (A) The heatmap of the expression values (FPKM [fragments per kilobase of transcript per million mapped reads] values in RNA sequencing analysis) of five candidate genes. FL, flag leaf; PE, peduncle; P, panicle. The S1 indicates booting stage, and S2 indicates 4 days after heading. (B) The expression level of *SbiHYZ.10G230700* at booting stage. (C) The expression level of *SbiHYZ.10G230700* at 4 days after heading. \*, \*\*, and \*\*\*Statistically significant differences at  $p < 0.05$ ,  $p < 0.01$ , and  $p < 0.001$  levels, respectively. ns denotes no statistically significant difference.

to the inhibition of the internal BR signaling pathway, which leads to the alleviation of feedback inhibition on BR biosynthetic enzymes and consequently results in an increase in BR synthesis. The elevated BR levels further inhibit auxin

biosynthesis, thereby reducing auxin concentrations. In future studies, we intend to apply BR through foliar spraying to mutant plants during the reproductive stage to validate our hypothesis.

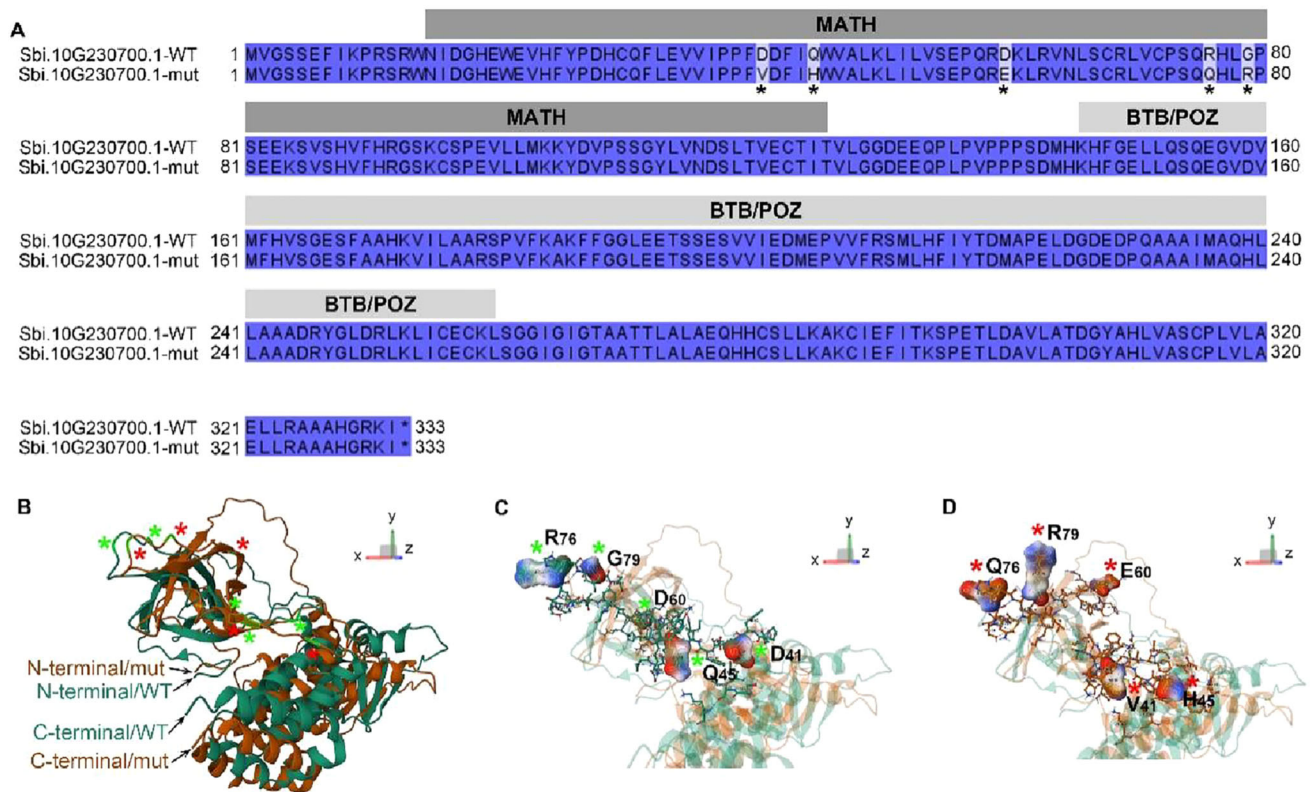


**FIGURE 6** Protein sequence analysis of SbiHYZ.10G230700 in wild type and mutant forms. (A) Amino acid sequence alignment of the SbiHYZ.10G230700 proteins in wild type (Sbi.10G230700-WT) and mutant (Sbi.10G230700-mut) variants. Amino acid residues highlighted indicate the non-synonymous mutant sites. The identical amino acid residues were present in a purple background. MATE and BTB/POZ represent the conserved MATE and BTB/POZ domains, respectively. (B) The 3D structure of the SbiHYZ.10G230700 protein monomer in wild type and mutant forms. The wild-type structure is depicted in green, while the mutant form is shown in red. (C) Close-up view of the surface topology at the residues corresponding to non-synonymous mutation sites from an identical perspective. (D) Close-up view of the surface topology at the non-synonymous mutation sites in the mutant SbiHYZ.10G230700 protein from an identical perspective. Green asterisks (\*) mark residues corresponding to non-synonymous mutation sites in the wild-type protein, and red asterisks (\*) denote the non-synonymous mutant residues in the mutant protein. The orientation axes for the protein 3D structures are displayed in the right-hand corners.

### 4.3 | Mapping of candidate regions for sorghum panicle exertion on Chromosome 10

Currently, a total of 42 QTLs related to sorghum panicle exertion have been detected across 10 chromosomes, with three QTLs mapped to chromosome 10 (Sakhi et al., 2013; Zhao et al., 2016). Zhao et al. (2016) performed GWAS analysis on a natural population of 351 Sorghum Association Panel lines and mapped a total of 14 QTLs for panicle exertion across chromosomes 1, 2, 3, 6, 7, 9, and 10. Among them, two QTLs on chromosome 10 were located in the 41.74–45.82 Mb and 55.84–55.94 Mb regions, respectively. However, the *shp-1* locus in this study was mapped to the interval of 59.65 Mb and 59.92 Mb. The QTL position in the 55.84–55.94 Mb regions of the BTx623 v3.1 genome was converted to the HYZ genome (Ding et al., 2024), spanning 57.93–58.03 Mb. The candidate region on the HYZ genome slightly deviates from the previously reported QTL interval on chromosome 10, likely due to low genomic

coverage of GWAS markers from GBS sequencing or the different reference used for analysis. Hence, we hypothesize that the two intervals may represent the same genomic region.

### 4.4 | The BPM domain-containing protein might play important roles in the sorghum panicle exertion

The BPM domain-containing protein is an integral part of the E3 ubiquitin ligase complex, which is pivotal in the signal transduction of phytohormones (H. Chen et al., 2018; Lin et al., 2020; Shang et al., 2024; Song et al., 2023; Yu & Xie, 2023). E3 ubiquitin ligases complex plays a crucial regulatory role in BR signaling by modulating the stability and function of key components in the pathway, such as the BR receptor BR11, through ubiquitination, thereby influencing the strength and spatial specificity of BR signaling. For

instance, studies have shown that the C3HC4-type RING E3 ubiquitin ligase DGS1 promotes the degradation of BR11 via ubiquitination, regulating the sensitivity of BR signaling (J. Li et al., 2023; X. Zhu et al., 2021). Further research has demonstrated that the function of E3 ubiquitin ligases is not limited to promoting protein degradation; they can also positively regulate BR signaling by interacting with the core transcription factor OsBZR1 to modulate the expression of downstream genes (X. Zhu et al., 2021). These findings reveal the multifaceted roles of E3 ubiquitin ligases complex in BR signal transduction and underscore their importance in plant developmental processes, including internode elongation, plant height regulation, and grain development (Niu et al., 2022; Song et al., 2023; X. Zhu et al., 2021; Yu & Xie, 2023).

In this study, protein encoded by the candidate gene *Sbi-HYZ.10G230700* belongs to the BPM domain-containing protein 1–6 (IPR045005) family and is component of the E3 ubiquitin ligase complex. The BTB domain in BPM domain-containing protein facilitates enzyme activation through forming complex with CUL3, whereas the MATH domain orchestrates substrate recognition for ubiquitin tagging, which is a critical domain for the function of BPM domain-containing protein-mediated substrate ubiquitination (Diop et al., 2023). In Arabidopsis, there are only six members, while the rice genome contains over 60 members of the MATH-BTB gene family (Gingerich et al., 2007; Juranić & Dresselhaus, 2014). Phylogenetic analysis indicates that the MATH-BTB gene family members in plants can be clustered into six branches, with all six MATH-BTB genes in Arabidopsis located within the same ancient core branch (Gingerich et al., 2007; Juranić & Dresselhaus, 2014). Similarly, sorghum contains 41 protein-coding MATH-BTB members and 27 pseudogenes, along with two genes encoding degenerated MATH-related domains (located at the C-terminal of the BTB motif) (Gingerich et al., 2007). These studies suggest that the MATH-BTB family in sorghum has undergone evolutionary dynamics similar to those of the MATH-BTB A1 subfamily in rice, exhibiting a certain level of complexity and diversity. In this study, we identified that the amino acid mutation sites in the proteins encoded by candidate gene are localized within the MATH domain. These alterations in amino acids may disrupt the recognition of target substrates by the complex, consequently compromising the ubiquitination function of the protein complex, which potentially results in the panicle exertion phenotype of *shp-I* mutant. In summary, we propose that the candidate gene is involved in the signal transduction of the plant hormone BR, regulating PE development. This lays the foundation for subsequent functional validation and provides necessary targets for future efforts to create varieties suitable for mechanized harvesting by employing molecular approaches to precisely manipulate the expression of this gene.

## AUTHOR CONTRIBUTIONS

**Jianling Ao:** Formal analysis; investigation; validation; writing—original draft. **Ruoruo Wang:** Formal analysis; visualization; writing—review and editing. **Wenzeng Li:** Formal analysis; investigation; writing—original draft. **Yanqing Ding:** Data curation; resources; software. **Jianxia Xu:** Investigation; resources. **Ning Cao:** Data curation. **Xu Gao:** Investigation. **Bin Cheng:** Data curation. **Degang Zhao:** Supervision. **Liyi Zhang:** Conceptualization; project administration; resources; supervision; validation; writing—review and editing.

## ACKNOWLEDGMENTS

The authors would like to appreciate the financial support received from Guizhou Provincial Basic Research Program (Natural Science) (QKH Basic-[2024]Youth 077), Guizhou Provincial Key Laboratory of Biotechnology Breeding for Special Minor Cereals (QKHPT[2025]026), Innovation Capacity Building Project of Guizhou Scientific Institutions (QKFQ[2022]007), Guizhou Academy of Agricultural Sciences Key Laboratory Project for Crop Gene Resources and Germplasm Innovation in Karst Mountain regions (QNKZZZY[2023]06), Innovation Capacity Building of Guizhou Province Breeding and Scientific Research Foundation Platform (QKHFQ[2022]014), and National Science Foundation by Guizhou Academy of Agricultural Sciences ([2022] 03).

## CONFLICT OF INTEREST STATEMENT

All authors declare no conflicts of interest.

## DATA AVAILABILITY STATEMENT

The datasets utilized in this research can be obtained from the corresponding author upon reasonable request.

## ORCID

Ruoruo Wang  <https://orcid.org/0000-0002-6294-9655>

Liyi Zhang  <https://orcid.org/0000-0002-7230-1326>

## REFERENCES

- Ashikari, M., Wu, J., Yano, M., Sasaki, T., & Yoshimura, A. (1999). Rice gibberellin-insensitive dwarf mutant gene *Dwarf 1* encodes the alpha-subunit of GTP-binding protein. *Proceedings of the National Academy of Sciences of the United States of America*, 96(18), 10284–10289. <https://doi.org/10.1073/pnas.96.18.10284>
- Baye, W., Xie, Q., & Xie, P. (2022). Genetic architecture of grain yield-related traits in sorghum and maize. *International Journal of Molecular Sciences*, 23(5), 2405. <https://doi.org/10.3390/ijms23052405>
- Bolger, A. M., Lohse, M., & Usadel, B. (2014). Trimmomatic: A flexible trimmer for Illumina sequence data. *Bioinformatics (Oxford, England)*, 30(15), 2114–2120. <https://doi.org/10.1093/bioinformatics/btu170>

- Chen, H., Ma, B., Zhou, Y., He, S.-J., Tang, S.-Y., Lu, X., Xie, Q., Chen, S.-Y., & Zhang, J.-S. (2018). E3 ubiquitin ligase SOR1 regulates ethylene response in rice root by modulating stability of Aux/IAA protein. *Proceedings of the National Academy of Sciences of the United States of America*, *115*(17), 4513–4518. <https://doi.org/10.1073/pnas.1719387115>
- Chen, H.-J., & Wang, S.-J. (2008). Molecular regulation of sink–source transition in rice leaf sheaths during the heading period. *Acta Physiologiae Plantarum*, *30*(5), 639–649. <https://doi.org/10.1007/s11738-008-0160-8>
- Chen, X., Hu, X., Jiang, J., & Wang, X. (2024). Functions and mechanisms of brassinosteroids in regulating crop agronomic traits. *Plant & Cell Physiology*, *65*, 1568–1580. <https://doi.org/10.1093/pcp/pcae044>
- Ding, Y., Cao, N., Zhou, L., Cheng, B., Gao, X., Wang, C., Zhou, G., & Zhang, L. (2020). Construction of EMS-induced mutant library and mutant screening in liquor-making waxy sorghum. *Journal of Southern Agriculture*, *51*(12), 2884–2891. <https://doi.org/10.3969/j.issn.2095-1191.2020.12.003>
- Ding, Y., Wang, Y., Xu, J., Jiang, F., Li, W., Zhang, Q., Yang, L., Zhao, Z., Cheng, B., Cao, N., Gao, X., Zhang, X., Zou, G., Yang, F., & Zhang, L. (2024). A telomere-to-telomere genome assembly of Hongyingzi, a sorghum cultivar used for Chinese Baijiu production. *The Crop Journal*, *12*(2), 635–640. <https://doi.org/10.1016/j.cj.2024.02.011>
- Diop, A., Pietrangeli, P., Nardella, C., Pennacchietti, V., Pagano, L., Toto, A., Di Felice, M., Di Matteo, S., Marcocci, L., Malagrino, F., & Gianni, S. (2023). Biophysical characterization of the binding mechanism between the MATH domain of SPOP and its physiological partners. *International Journal of Molecular Sciences*, *24*(12), 10138. <https://doi.org/10.3390/ijms241210138>
- Duan, Y.-L., Guan, H.-Z., Zhuo, M., Chen, Z.-W., Li, W.-T., Pan, R.-S., Mao, D.-M., Zhou, Y.-C., & Wu, W.-R. (2012). Genetic analysis and mapping of an enclosed panicle mutant locus esp1 in rice (*Oryza sativa* L.). *Journal of Integrative Agriculture*, *11*(12), 1933–1939. [https://doi.org/10.1016/s2095-3119\(12\)60449-3](https://doi.org/10.1016/s2095-3119(12)60449-3)
- Felderhoff, T. J., Murray, S. C., Klein, P. E., Sharma, A., Hamblin, M. T., Kresovich, S., Vermerris, W., & Rooney, W. L. (2012). QTLs for energy-related traits in a sweet × Grain Sorghum [*Sorghum bicolor* (L.) Moench] mapping population. *Crop Science*, *52*(5), 2040–2049. <https://doi.org/10.2135/cropsci2011.11.0618>
- Feltus, F., Hart, G., Schertz, K., Casa, A., Kresovich, S., Abraham, S., Klein, P., Brown, P., & Paterson, A. (2006). Alignment of genetic maps and QTLs between inter- and intra-specific sorghum populations. *Theoretical and Applied Genetics*, *112*, 1295–1305. <https://doi.org/10.1007/s00122-006-0232-3>
- Friedrichsen, D., & Chory, J. (2001). Steroid signaling in plants: From the cell surface to the nucleus. *BioEssays: News and reviews in molecular, cellular and developmental biology*, *23*, 1028–1036. <https://doi.org/10.1002/bies.1148>
- Fu, B., Ma, J., Cheng, Z., Chen, J., Shen, J., Zhang, B., Ren, Y., Ding, Y., Zhou, Y., Zhang, H., Zhou, K., Wang, J.-L., Lei, C., Zhang, X., Guo, X., Gao, H., Bao, Y., & Wan, J.-M. (2016). Phosphatidylserine synthase controls cell elongation especially in the uppermost internode in rice by regulation of exocytosis. *PLoS One*, *11*(4), e0153119. <https://doi.org/10.1371/journal.pone.0153119>
- Fuyao, Z., Junai, P., & Weijun, Z. (2019). Genetic quality improvement of brewing sorghum in China: Research progress. *Journal of Agriculture*, *9*(3), 21–25. <https://doi.org/10.11923/j.issn.2095-4050.cjas18030019>
- Gingerich, D. J., Hanada, K., Shiu, S. H., & Vierstra, R. D. (2007). Large-scale, lineage-specific expansion of a bric-a-brac/tramtrack/broad complex ubiquitin-ligase gene family in rice. *The Plant Cell*, *19*, 2329–2348. <https://doi.org/10.1105/tpc.107.051300>
- Girma, G., Nida, H., Seyoum, A., Mekonen, M., Nega, A., Lule, D., Dessalegn, K., Bekele, A., Gebreyohannes, A., Adeyanju, A., Tirfessa, A., Ayana, G., Taddese, T., Mekbib, F., Belete, K., Tesso, T., Ejeta, G., & Mengiste, T. (2019). A large-scale genome-wide association analyses of Ethiopian sorghum landrace collection reveal loci associated with important traits. *Frontiers in Plant Science*, *10*, Article 691. <https://doi.org/10.3389/fpls.2019.00691>
- Guan, H. Z., Duan, Y. L., Liu, H. Q., Chen, Z. W., Zhuo, M., Zhuang, L. J., Qi, W. M., Pan, R. S., Mao, D. M., Zhou, Y. C., Wang, F., & Wu, W. R. (2011). Genetic analysis and fine mapping of an enclosed panicle mutant esp2 in rice (*Oryza sativa* L.). *Chinese Science Bulletin*, *56*(14), 1476–1480. <https://doi.org/10.1007/s11434-011-4552-9>
- Guo, F., Lv, M., & Li, J. (2023). Current progress on the regulation of brassinosteroid homeostasis and signal transduction. *Plant Physiology Journal*, *59*(12), 2217–2240. <https://doi.org/10.13592/j.cnki.ppj.400012>
- Guo, F., Lv, M., Zhang, J., & Li, J. (2024). Crosstalk between brassinosteroids and other phytohormones during plant development and stress adaptation. *Plant And Cell Physiology*, *65*, 1530–1543. <https://doi.org/10.1093/pcp/pcae047>
- Halliday, K. J. (2004). Plant hormones: The interplay of brassinosteroids and auxin. *Current Biology*, *14*, R1008–R1010. <https://doi.org/10.1016/j.cub.2004.11.025>
- He, J.-X., Gendron, J. M., Sun, Y., Gampala, S. S. L., Gendron, N., Sun, C. Q., & Wang, Z.-Y. (2005). BZR1 Is a transcriptional repressor with dual roles in brassinosteroid homeostasis and growth responses. *Science*, *307*, 1634–1638. <https://doi.org/10.1126/science.1107580>
- Jian, M., Min, S., Puyang, D., Wei, L., Xiaohong, Z., Congcong, Y., Han, Z., Nana, Q., Yujie, Y., & Xiujin, L. (2017). Genetic identification of QTL for neck length of spike in wheat. *Journal of Triticeae Crops*, *37*(3), 319–324. <https://doi.org/10.7606/j.issn.1009-1041.2017.03.06>
- Jumper, J., Evans, R., Pritzel, A., Green, T., Figurnov, M., Ronneberger, O., Tunyasuvunakool, K., Bates, R., Židek, A., Potapenko, A., Bridgland, A., Meyer, C., Kohl, S. A. A., Ballard, A. J., Cowie, A., Romera-Paredes, B., Nikolov, S., Jain, R., Adler, J., ... Hassabis, D. (2021). Highly accurate protein structure prediction with AlphaFold. *Nature*, *596*(7873), 583–589. <https://doi.org/10.1038/s41586-021-03819-2>
- Juranić, M., & Dresselhaus, T. (2014). Phylogenetic analysis of the expansion of the MATH-BTB gene family in the grasses. *Plant Signaling & Behavior*, *9*, e28242. <https://doi.org/10.4161/psb.28242>
- Kim, D., Paggi, J. M., Park, C., Bennett, C., & Salzberg, S. L. (2019). Graph-based genome alignment and genotyping with HISAT2 and HISAT-genotype. *Nature Biotechnology*, *37*(8), 907–915. <https://doi.org/10.1038/s41587-019-0201-4>
- Kun, W. (2009). *Genetic analysis and gene mapping of rice Dwarf and sheathed panicle mutant dsp1*. Yangzhou University.
- Li, C., Tang, H., Luo, W., Zhang, X., Mu, Y., Deng, M., Liu, Y., Jiang, Q., Chen, G., Wang, J., Qi, P., Pu, Z., Jiang, Y., Wei, Y., Zheng, Y., Lan, X., & Ma, J. (2020). A novel, validated, and plant height-independent QTL for spike extension length is associated with yield-related traits in wheat. *Theoretical and Applied Genetics*, *133*(12), 3381–3393. <https://doi.org/10.1007/s00122-020-03675-0>
- Li, J., Zhang, B., Duan, P., Yan, L., Yu, H., Zhang, L., Li, N., Zheng, L., Chai, T., Xu, R., & Li, Y. (2023). An endoplasmic reticulum-

- associated degradation-related E2-E3 enzyme pair controls grain size and weight through the brassinosteroid signaling pathway in rice. *The Plant Cell*, 35, 1076–1091. <https://doi.org/10.1093/plcell/koac364>
- Lin, Q., Zhang, Z., Wu, F., Feng, M., Sun, Y., Chen, W., Cheng, Z., Zhang, X., Ren, Y., Lei, C., Zhu, S., Wang, J., Zhao, Z., Guo, X., Wang, H., & Wan, J. (2020). The APC/CTE E3 ubiquitin ligase complex mediates the antagonistic regulation of root growth and tillering by ABA and GA. *The Plant Cell*, 32(6), 1973–1987. <https://doi.org/10.1105/tpc.20.00101>
- Luo, A., Qian, Q., Yin, H., Liu, X., Yin, C., Lan, Y., Tang, J., Tang, Z., Cao, S., Wang, X., Xia, K., Fu, X., Luo, D., & Chu, C. (2006). EUI1, encoding a putative cytochrome P450 monooxygenase, regulates internode elongation by modulating gibberellin responses in rice. *Plant and Cell Physiology*, 47(2), 181–191. <https://doi.org/10.1093/pcp/pci233>
- McKenna, A., Hanna, M., Banks, E., Sivachenko, A., Cibulskis, K., Kernysky, A., Garimella, K., Altshuler, D., Gabriel, S., Daly, M., & DePristo, M. A. (2010). The genome analysis toolkit: A mapreduce framework for analyzing next-generation DNA sequencing data. *Genome Research*, 20, 1297–1303. <https://doi.org/10.1101/gr.107524.110>
- McKim, S. M. (2019). How plants grow up. *Journal of Integrative Plant Biology*, 61(3), 257–277. <https://doi.org/10.1111/jipb.12786>
- Mei, E., He, M., Xu, M., Tang, J., Liu, J., Liu, Y., Hong, Z., Li, X., Wang, Z., Guan, Q., Tian, X., & Bu, Q. (2024). OsWRKY78 regulates panicle exertion via gibberellin signaling pathway in rice. *Journal of Integrative Plant Biology*, 66(4), 771–786. <https://doi.org/10.1111/jipb.13636>
- Murray, M. G., & Thompson, W. F. (1980). Rapid isolation of high molecular weight plant DNA. *Nucleic Acids Research*, 8(19), 4321–4326. <https://doi.org/10.1093/nar/8.19.4321>
- Niu, M., Wang, H., Yin, W., Meng, W., Xiao, Y., Liu, D., Zhang, X., Dong, N., Liu, J., Yang, Y., Zhang, F., Chu, C., & Tong, H. (2022). Rice DWARF AND LOW-TILLERING and the homeodomain protein OSH15 interact to regulate internode elongation via orchestrating brassinosteroid signaling and metabolism. *The Plant Cell*, 34, 3754–3772. <https://doi.org/10.1093/plcell/koac196>
- Perez, M. B. M., Zhao, J., Yin, Y. H., Hu, J. Y., & Fernandez, M. G. S. (2014). Association mapping of brassinosteroid candidate genes and plant architecture in a diverse panel of. *Theoretical and Applied Genetics*, 127(12), 2645–2662. <https://doi.org/10.1007/s00122-014-2405-9>
- Qi, S., Zhichao, Z., Jinhui, Z., Feng, Z., Zhijun, C., & Detang, Z. (2020). Genetic analysis and fine mapping of a sheathed panicle mutant *sui2* in rice (*Oryza sativa* L.). *Acta Agronomica Sinica*, 46(11), 1734–1742. <https://doi.org/10.3724/SP.J.1006.2020.02009>
- Rao, X., & Dixon, R. A. (2017). Brassinosteroid mediated cell wall remodeling in grasses under abiotic stress. *Frontiers in Plant Science*, 8, 806. <https://doi.org/10.3389/fpls.2017.00806>
- Rutger, J., & Carnahan, H. (1981). A fourth genetic element to facilitate hybrid cereal production—A recessive tall in rice 1. *Crop Science*, 21(3), 373–376. [10.2135/cropsci1981.0011183X002100030005x](https://doi.org/10.2135/cropsci1981.0011183X002100030005x)
- Sakhi, S., Shehzad, T., Rehman, S., & Okuno, K. (2013). Mapping the QTLs underlying drought stress at developmental stage of sorghum (*Sorghum bicolor* (L.) Moench) by association analysis. *Euphytica*, 193(3), 433–450. <https://doi.org/10.1007/s10681-013-0963-6>
- Shang, E., Wei, K., Lv, B., Zhang, X., Lin, X., Ding, Z., Leng, J., Tian, H., & Ding, Z. (2024). VIK-mediated auxin signaling regulates lateral root development in *Arabidopsis*. *Advanced Science*, 11(33), 2402442. <https://doi.org/10.1002/adv.202402442>
- Shefflin, A. M., Kirkwood, J. S., Wolfe, L. M., Jahn, C. E., Broeckling, C. D., Schachtman, D. P., & Prenni, J. E. (2019). High-throughput quantitative analysis of phytohormones in sorghum leaf and root tissue by ultra-performance liquid chromatography-mass spectrometry. *Analytical and Bioanalytical Chemistry*, 411, 4839–4848. <https://doi.org/10.1007/s00216-019-01658-9>
- Shubiao, Z., RenCui, Y., Ronghua, H., & Qingqi, Z. (2005). Achievement in rice *eui* gene and *eui* hybrids Studies. *Southwest China Journal of Agricultural Sciences*, 5, 166–172. <https://doi.org/10.16213/j.cnki.scjas.2005.05.035>
- Shunguo, L., Meng, L., Fei, L., Jianqiu, Z., Xiaochun, L., & Xian, D. (2021). Current status and future prospective of sorghum production and seed industry in China. *Scientia Agricultura Sinica*, 54(3), 471–482. <https://doi.org/10.3864/j.issn.0578-1752.2021.03.002>
- Si, X. M., Wang, W. X., Wang, K., Liu, Y. C., Bai, J. P., Meng, Y. X., Zhang, X. Y., & Liu, H. X. (2021). A sheathed spike gene, inhibits stem elongation in common wheat by regulating hormone levels. *International Journal of Molecular Sciences*, 22(20), 11210. <https://doi.org/10.3390/ijms222011210>
- Song, L., Liu, J., Cao, B., Liu, B., Zhang, X., Chen, Z., Dong, C., Liu, X., Zhang, Z., Wang, W., Chai, L., Liu, J., Zhu, J., Cui, S., He, F., Peng, H., Hu, Z., Su, Z., Guo, W., ... Ni, Z. (2023). Reducing brassinosteroid signalling enhances grain yield in semi-dwarf wheat. *Nature*, 617(7959), 118–124. <https://doi.org/10.1038/s41586-023-06023-6>
- Trapnell, C., Roberts, A., Goff, L., Pertea, G., Kim, D., Kelley, D. R., Pimentel, H., Salzberg, S. L., Rinn, J. L., & Pachter, L. (2012). Differential gene and transcript expression analysis of RNA-seq experiments with TopHat and Cufflinks. *Nature Protocols*, 7(3), 562–578. <https://doi.org/10.1038/nprot.2012.016>
- Tanaka, K., Asami, T., Yoshida, S., Nakamura, Y., Matsuo, T., & Okamoto, S. (2005). Brassinosteroid homeostasis in *Arabidopsis* is ensured by feedback expressions of multiple genes involved in its metabolism. *Plant Physiology*, 138, 1117–1125. <https://doi.org/10.1104/pp.104.058040>
- Tian, H., Lv, B., Ding, T., Bai, M., & Ding, Z. (2018). Auxin-BR interaction regulates plant growth and development. *Frontiers in Plant Science*, 8, 2256. <https://doi.org/10.3389/fpls.2017.02256>
- Tong, H., & Chu, C. (2018). Functional specificities of brassinosteroid and potential utilization for crop improvement. *Trends in Plant Science*, 23(11), 1016–1028. <https://doi.org/10.1016/j.tplants.2018.08.007>
- Wang, D. R., Wolfrum, E. J., Virk, P., Ismail, A., Greenberg, A. J., & McCouch, S. R. (2016). Robust phenotyping strategies for evaluation of stem non-structural carbohydrates (NSC) in rice. *Journal of Experimental Botany*, 67(21), 6125–6138. <https://doi.org/10.1093/jxb/erw375>
- Wu, L., Cui, Y., Xu, Z., & Xu, Q. (2020). Identification of multiple grain shape-related loci in rice using bulked segregant analysis with high-throughput sequencing. *Frontiers in Plant Science*, 11, 303. <https://doi.org/10.3389/fpls.2020.00303>
- Xiong, Y., Wu, B., Du, F., Guo, X., Tian, C., Hu, J., Lü, S., Long, M., Zhang, L., Wang, Y., & Jiao, Y. (2021). A crosstalk between auxin and brassinosteroid regulates leaf shape by modulating growth anisotropy. *Molecular Plant*, 14, 949–962. <https://doi.org/10.1016/j.molp.2021.03.011>
- Yamamuro, C., Ihara, Y., Wu, X., Noguchi, T., Fujioka, S., Takatsuto, S., Ashikari, M., Kitano, H., & Matsuoka, M. (2000). Loss of function of

- a rice brassinosteroid insensitive1 homolog prevents internode elongation and bending of the lamina joint. *The Plant Cell*, *12*, 1591–1606. <https://doi.org/10.1105/tpc.12.9.1591>
- Ye, Y., Qi, S., Xinxin, X., Haitao, Z., ZhiChao, Z., & Zhijun, C. (2023). Identification of sheathed panicle mutant *sui1-5* and screening of OsPSS1 interaction protein in rice (*Oryza sativa* L.). *Acta Agronomica Sinica*, *49*(03), 597–607. <https://doi.org/10.3724/SP.J.1006.2023.22014>
- Yin, C., Gan, L., Ng, D., Zhou, X., & Xia, K. (2007). Decreased panicle-derived indole-3-acetic acid reduces gibberellin A1 level in the uppermost internode, causing panicle enclosure in male sterile rice Zhenshan 97A. *Journal of Experimental Botany*, *58*(10), 2441–2449. <https://doi.org/10.1093/jxb/erm077>
- Yin, H. F., Gao, P., Liu, C. W., Yang, J., Liu, Z. C., & Luo, D. (2013). SUI-family genes encode phosphatidylserine synthases and regulate stem development in rice. *Planta*, *237*(1), 15–27. <https://doi.org/10.1007/s00425-012-1736-5>
- Yu, F., & Xie, Q. (2023). ER-associated ubiquitin-conjugating enzyme: A key regulator of grain yield and stress resistance in crops. *Trends in Plant Science*, *29*(3), 286–289. <https://doi.org/10.1016/j.tplants.2023.11.025>
- Zhang, H., Wang, X., Pan, Q., Li, P., Liu, Y., Lu, X., Zhong, W., Li, M., Han, L., Li, J., Wang, P., Li, D., Liu, Y., Li, Q., Yang, F., Zhang, Y. M., Wang, G., & Li, L. (2019). QTG-seq accelerates QTL fine mapping through QTL partitioning and whole-genome sequencing of bulked segregant samples. *Molecular Plant*, *12*, 426–437. <https://doi.org/10.1016/j.molp.2018.12.018>
- Zhao, J., Mantilla Perez, M. B., Hu, J., & Salas Fernandez, M. G. (2016). Genome-wide association study for nine plant architecture traits in sorghum. *The Plant Genome*, *9*(2), plantgenome2015.06.0044. <https://doi.org/10.3835/plantgenome2015.06.0044>
- Zhihong, D., Fuyao, Z., Junai, P., Xin, L., Huiming, L., & Tingting, Y. (2014). Discussion on development of mechanization of sorghum industry. *Modern Agricultural Science and Technology*, *24*, 87–88. <https://link.cnki.net/urlid/34.1278.s.20150113.1724.006>
- Zhu, X., Zhang, S., Chen, Y., Mou, C., Huang, Y., Liu, X., Ji, J., Yu, J., Hao, Q., Yang, C., Cai, M., Nguyen, T., Song, W., Wang, P., Dong, H., Liu, S., Jiang, L., & Wan, J. (2021). Decreased grain size1, a C3HC4-type RING protein, influences grain size in rice (*Oryza sativa* L.). *Plant Molecular Biology*, *105*, 405–417. <https://doi.org/10.1007/s11103-020-01096-7>
- Zhu, Y., Nomura, T., Xu, Y., Zhang, Y., Peng, Y., Mao, B., Hanada, A., Zhou, H., Wang, R., Li, P., Zhu, X., Mander, L. N., Kamiya, Y., Yamaguchi, S., & He, Z. (2006). ELONGATED UPPERMOST INTERNODE encodes a cytochrome P450 monooxygenase that epoxidizes gibberellins in a novel deactivation reaction in rice. *The Plant Cell*, *18*(2), 442–456. <https://doi.org/10.1105/tpc.105.038455>
- Zou, Q., Tu, R., Wu, J., Huang, T., Sun, Z., Ruan, Z., Cao, H., Yang, S., Shen, X., He, G., & Wang, H. (2024). A polygalacturonase gene *OsPG1* modulates water homeostasis in rice. *The Crop Journal*, *12*(1), 79–91. <https://doi.org/10.1016/j.cj.2023.12.007>

## SUPPORTING INFORMATION

Additional supporting information can be found online in the Supporting Information section at the end of this article.

**How to cite this article:** Ao, J., Wang, R., Li, W., Ding, Y., Xu, J., Cao, N., Gao, X., Cheng, B., Zhao, D., & Zhang, L. (2025). Gene mapping and candidate gene analysis of a sorghum *sheathed panicle-I* mutant. *The Plant Genome*, *18*, e70007. <https://doi.org/10.1002/tpg2.70007>